ELSEVIER

Journal of Molecular Catalysis B: Enzymatic 10 (2000) 453–469

JOURNAL OF MOLECULAR CATALYSIS B: ENZYMATIC

www.elsevier.com/locate/molcatb

Cytochrome *c* immobilization into mesoporous molecular sieves

Lisa Washmon-Kriel, Victoria L. Jimenez, Kenneth J. Balkus Jr.*

Department of Chemistry, University of Texas at Dallas, Richardson, TX 75083-0688, USA

Received 23 August 1999; received in revised form 22 October 1999; accepted 10 December 1999

Abstract

The immobilization of cytochrome *c* into the mesoporous moleclar sieves MCM-48 (Mobil Composition of Matter) and SBA-15 (Santa Barbara Amorphous), as well as the layered niobium oxide Nb-TMS4 (Niobium Transition Metal Oxide Molecular Sieve) is described. The cytochrome *c* loading was influenced by the molecular sieve structure, i.e., one-dimensional vs. three-dimensional. Cytochrome *c* immobilization was accomplished by absorption into the molecular sieves followed by silylation of the pore openings. The molecular sieves containing cytochrome *c* were characterized by X-ray diffraction (XRD), scanning electron microscopy (SEM), UV/Vis, and FT-IR spectroscopy. The protein was found to be stable in the molecular sieve under conditions that would denature the protein in solution. The immobilized cytochrome *c* retained its redox activity following immobilization for several months as demonstrated by cyclic voltammetry (CV).

Keywords: Mesoporous molecular sieves; Enzyme immobilization; Cytochrome *c*; MCM-48; SBA-15; Nb-TMS4

1. Introduction

We recently reported the application of mesoporous molecular sieves as host materials for the immobilization of proteins and enzymes [1,2]. The immobilization of small biomolecules by absorption and silylation in mesoporous molecular sieves or layered materials may offer advantages over traditional methods such as covalent binding, membrane encapsulation, cross-linking, and sol–gel entrapment [3]. Mesoporous molecular sieves are available in one- to three-dimensional channel systems having uniform pores in the range of 20–300 Å. These host materials can be prepared in a variety of compositions including transition metal oxides. Additionally, these metal oxide supports are chemically inert and stable at elevated temperatures. The uniform pore structure of mesoporous molecular sieves is an improvement over amorphous sol–gel derived materials that generally exhibit a fairly broad pore distribution. The uniform pores of molecular sieve materials allow for control of molecular absorption on the basis of size. Enclosure of the protein in a well-defined space may also help prevent protein denaturing. Additionally, the pore structure may be systematically varied, which may provide insight into changes in the tertiary structure and active site during catalysis. We have previously reported the immobilization of small biomolecules such as trypsin, papain, and cy-

* Corresponding author.
E-mail address: balkus@utdallas.edu (K.J. Balkus).

1381-1177/00/$ - see front matter
PII: S1381-1177(99)00123-X

tochrome *c* in hexagonal MCM-41 (Mobil Composition of Matter) [2] and Nb-TMS1 (Niobium Transition Metal Oxide Molecular Sieve) [1] mesoporous molecular sieves, whose structures consist of one-dimensional channels running in parallel. The enzymes trypsin and papain were readily absorbed into the pores of template-free all silica MCM-41.This immobilization into MCM-41 improved enzyme stability, however, the observed catalytic activity of trypsin and papain was not dramatically improved compared with other support materials [2]. This may be the result of the one-dimensional MCM-41 pore system where access to the occluded biomolecules may be limited to the ends of the channels. This encouraged us to examine immobilization of the protein cytochrome *c* into MCM-48, a mesoporous mole-

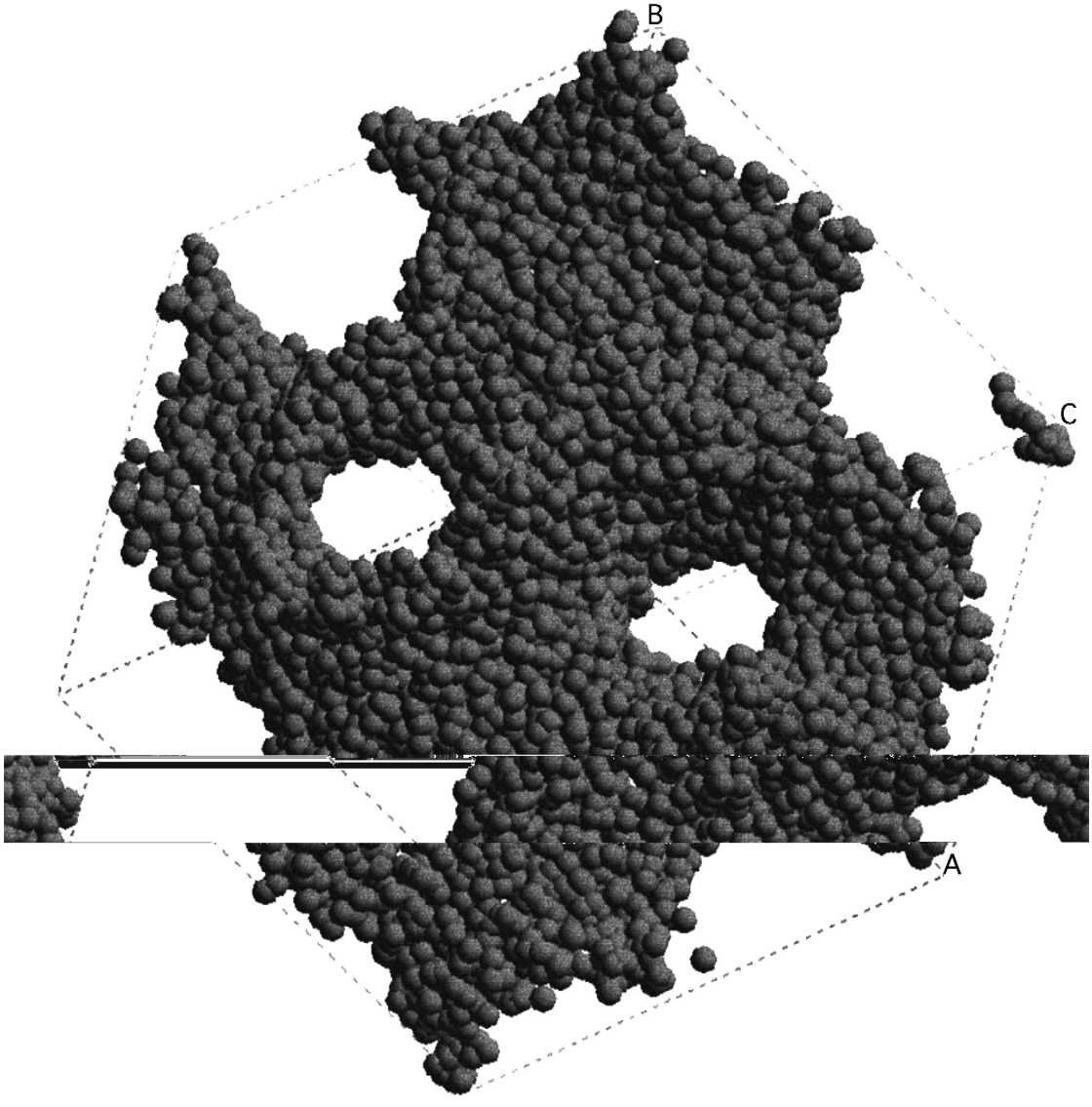

Fig. 1. Calculated structure of MCM-48, the cubic M41S material consisting of two non-intersecting pore systems [9].

cular sieve having a three-dimensional pore structure available in the range of ~20–40 Å [4–7]. MCM-48 is the cubic member of the M41S family of mesoporous molecular sieves reported by Mobil in 1992 [8], as shown in Fig. 1 [9]. MCM-48 contains two non-intersecting pore systems, and the pores are accessible from all sides, compared to the one-dimensional pores of MCM-41. The immobilization and characterization of encapsulated cytochrome *c* in mesoporous MCM-48 is presented below. The Fe(II)/(III) couple associated with the heme group at the active site is conveniently monitored by cyclic voltammetry (CV). Although electrochemistry of intrazeolite complexes is well known, the redox accessible protein is probably limited to pore openings of the insulating MCM-48. The compositional variance available to mesoporous molecular sieves and layered materials includes semiconducting and conducting metal oxides. Such mesophases might facilitate characterization of the encapsulated proteins. We have previously studied Nb-TMS1 that has the same limitations as MCM-41, therefore, we have also examined a layered niobium oxide, Nb-TMS4 [10], as a host matrix for cytochrome *c*. Mesophase transition metal hosts of this type might facilitate the electron transfer process. This aspect could be further exploited in applications for the molecular sieve encapsulated proteins such as in the area of biosensors and catalysis [11]. Another feature of materials like Nb-TMS4 is the possible octahedral coordination of niobium such that basic functional groups on the protein surface might bind to the niobium oxide pore walls. The preparation and characterization of Nb-TMS4 supported cytochrome *c* is also described below.

With the advent of ultra large pore mesoporous materials such as SBA-15 (Santa Barbara Amorphous) [12] it is also possible to use this technique to investigate immobilization of larger proteins and enzymes as well as compare the absorption of a relatively small protein such as cytochrome *c* into different pore size materials. SBA-15 is an all silica mesoporous molecular sieve possessing one-dimensional hexagonal channels with pore diameters that have been reported in the range of 50–300 Å. We also report preliminary work using SBA-15 for the encapsulation of cytochrome *c*.

2. Experimental

2.1. General techniques

Powder X-ray diffraction (XRD) patterns were obtained with a Scintag XDS 2000 X-ray diffractometer using CuKα radiation. Infrared spectra were acquired from KBr pellets with a Nicolet Avatar 360 FT-IR spectrophotometer. Scanning electron micrographs were obtained from Pd/Au coated samples using a Phillips 60XL LaB_6 microscope. Solution UV/Vis spectra were collected on a Shimadzu UV-1601PC spectrophotometer. Single point BET surface areas were calculated using a Micromeritics Flowsorb II 200 instrument. Argon isotherms were measured at 77 K using a volumetric gas adsorption apparatus built in-house. CV of the protein immobilized in the molecular sieves was conducted at room temperature using an EG and G Princeton Applied Research VERSASTAT potentiostat. The electrochemistry experiments were conducted using a standard three electrode cell, in a solution comprised of pH 7.0 potassium phoshpate monobasic-hydroxide buffer 0.05 M (Fisher), sodium perchlorate (Fisher), and 4-4′-bipyridyl (Aldrich), as a mediator. Electrode potentials were referenced to a Ag/AgCl electrode and a platinum wire was used as the counter electrode. The working electrode was prepared by mixing the silanted molecular sieve containing cytochrome *c* with an equal amount (w/w) of graphite and subsequently pressing (15,000 psig) the mixture onto ~3 cm^2 platinum gauze (100 mesh, Aldrich), as previously reported [13]. The preparation of the electrode in such a manner does not result in a loss of molecular sieve crystallinity as evidenced by powder XRD.

2.2. Materials

All silica MCM-48 molecular sieves were synthesized according to a published procedure [14], followed by a post-hydrothermal treatment to yield a very highly ordered material [15]. A clear solution of 10% (w/w) cetyltrimethylammonium bromide (CTAB) solution (27.8 g total weight) was prepared in a 125-ml Teflon bottle. While stirring continuously, 3.3 ml of 2 N sodium hydroxide solution and 3.3 ml of a tetraethylorthosilicate (TEOS) (Aldrich 98%) solution were added, sequentially. The resulting transparent solution was covered and stirred at room temperature for 30 min. After 5 min of stirring, a precipitate formed. The synthesis gel, having a molar ratio of $1SiO_2$:$0.23Na_2O$:0.55CTAB:$112H_2O$, was heated at 100°C under static conditions for 2 days. The resulting white product was collected by filtration, washed with 100–200 ml deionized water, then returned to the Teflon bottle and heated at 100°C for 24 h after replacing the mother liquor with deionized water (10 ml for each gram of air-dried as-synthesized product). The highly ordered MCM-48 material was washed with copious amounts of deionized water and air-dried at room temperature overnight. The organic template was removed by calcination at 540°C for 16 h.

The transition metal oxide Nb-TMS4 was synthesized using a variation of a published procedure [10]. In our Nb-TMS4 synthesis, 0.344 g of octadecylamine (97% Aldrich) and 1.0 g niobium (V) ethoxide (99.99% Chemat Technology) were melted together at 50°C in a plastic beaker. Upon cooling, 10 ml of absolute ethanol was added, followed by 10 ml of deionized water. The white precipitate was aged in the supernatant 72 h at room temperature prior to heating statically in a Teflon lined 45 ml Parr stainless steel autoclave at two different reaction temperatures. The Nb-TMS4 synthesis gel was first heated at 90°C for 24 h and then heated for 6 days at 180°C. The white product was collected by suction filtration and washed with deionized water, and 200 ml of ethanol, followed by 200 ml of diethyl ether. Template removal was performed by ethanolic acid extraction. As-synthesized Nb-TMS4 was stirred in 200 ml of a 4:1 isopropanol:water solution brought to pH 5 with nitric acid for 24 h at 80°C, followed by washing with 400 ml of deionized water and 400 ml of absolute ethanol until a pH of 7 was reached. The resulting extracted Nb-TMS4 was air-dried at room temperature overnight.

SBA-15-type molecular sieves can be synthesized using Pluronic® or Pluronic® R[1] block copolymer non-ionic surfactants [10,16]. The copolymer is comprised of alternating ethylene oxide and propylene oxide blocks. In this work, SBA-15 was synthesized by dissolving 0.0348 g P123 ($EO_{20}PO_{70}EO_{20}$, a Pluronic® block copolymer) in 30 ml of deionized water at room temperature. Subsequently, 1.8 ml aqueous concentrated HCl (EM Science) were added dropwise followed by the addition of 2.122 g TEOS. The clear solution, having a molar composition of $1SiO_2$:$6HCl$:$167H_2O$:0.0004P123, was covered and stirred for 20 min, transferred to a 125-ml polypropylene bottle, capped and heated at 35°C for 20 h, followed by heating at 100°C for 24 h. The resulting white product was washed with deionized water and dried in air at room temperature. The Pluronic template was removed by calcination in air at 500°C for 14 h. The resulting highly ordered SBA-15 was characterized by powder XRD, scanning electron microscopy (SEM), and argon adsorption isotherms. SEM revealed the expected rope-like morphology of SBA-15 [16] approximately 1 μm in length.

2.3. Cytochrome c encapsulation

Horse heart ferricytochrome *c* (Sigma) was purified according to a published method [17].

[1] Pluronic poly(alkylene oxide) triblock copolymers are a registered product of BASF, Mount Olive, NJ.

Ferricyanide was employed to insure the protein was in the oxidized form. Cytochrome *c* was eluted by gradient chromatography from a cellulose column using 50–90 mM pH 7 phosphate solutions. Fractions were collected at 3-ml intervals and analyzed by UV/Vis spectroscopy. The fractions of interest were subjected to dialysis, and the resulting purified cytochrome *c* was lyophilized. Cytochrome *c* was absorbed into template-free MCM-48 and SBA-15 and acid extracted Nb-TMS4 by stirring 50–150 mg molecular sieve in 5.0 ml of a 15–100-μM cytochrome *c* solution (pH 6.0 phosphate buffer) in a centrifuge tube. The mixture was stirred at 4°C for 2 h. The molecular sieve was collected by centrifugation (approximately 5 min), and the supernatant was subjected to UV/Vis spectroscopy following filtration through a 0.45-μm Teflon syringe filter (Whatman). Cytochrome *c* loading was determined by monitoring the change in the strong absorption band at 409 nm ($\varepsilon = 92000\ M^{-1}\ cm^{-1}$) and/or the weaker band at 530 nm ($\varepsilon = 9500\ M^{-1}\ cm^{-1}$).

It has been previously observed that following entrapment, cytochrome *c* can be desorbed from molecular sieve materials at or above the protein isoelectric point [2] (pH 10 for cytochrome *c*) [18]. However, cytochrome *c* can be immobilized by silylation of the pore openings which effectively blocks the pore apertures. Organisilane functionalization of MCM-41 has been used for a variety of purposes including the reduction of pore size [19–21], and has been well documented in the literature [22–29]. The pore openings and external surfaces of the MCM-48, Nb-TMS4, and SBA-15 containing cytochrome *c* were silylated by stirring approximately 300 mg of the mesoporous molecular sieves in 50 ml dry dichloromethane, 2.5 ml of 2,6-lutidine, and 1 ml 4-(trichlorosilyl)butyronitrile (Aldrich) at 0°C under a flow of nitrogen for 3 h, then stirred under a blanket of nitrogen overnight. The silane functionalized products were washed with dichloromethane, pH 6 phosphate buffer solution, deionized water, and air-dried at room temperature. Removal of any cytochrome *c* adsorbed to exterior surfaces or from pores that had not been fully silylated was carried out by stirring a small amount of the molecular sieve/cytochrome *c* complex (100 mg) in 5 ml of pH 10 (0.05 M) buffer (Fisher) for 24 h. The samples were centrifuged, the supernatant filtered through a 0.45-μm syringe filter and analyzed by UV/Vis spectroscopy. This process was repeated until no cytochrome *c* was detected in the supernatant.

3. Results and discussion

3.1. Molecular sieve characterization

Highly ordered MCM-48 was synthesized having pores on the order of 32–35 Å in diameter (calculated from *d* spacing). The XRD patterns of the as-synthesized and calcined MCM-48 are shown in Fig. 2, where at least four reflections are readily observed, including the (211), (200, (420), and the (332) reflections. Upon calcination of the as-synthesized material, broadening of the (211) peak is observed as well as a small contraction of the unit cell (~3 Å). Fig. 3 shows a typical TEM image of as-synthesized MCM-48 revealing the well-ordered pore structure [30]. The use of a post-

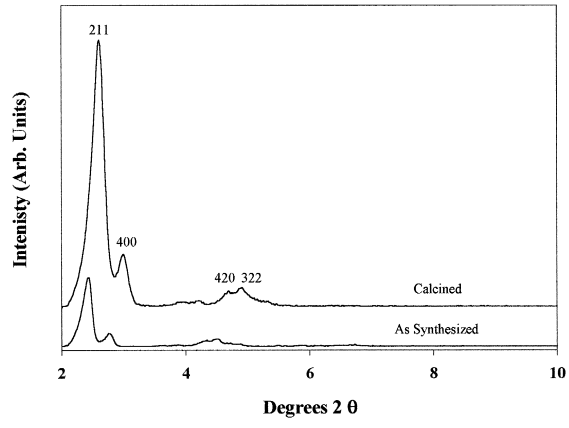

Fig. 2. Powder XRD pattern of (a) as-synthesized and (b) calcined hydrothermally synthesized MCM-48.

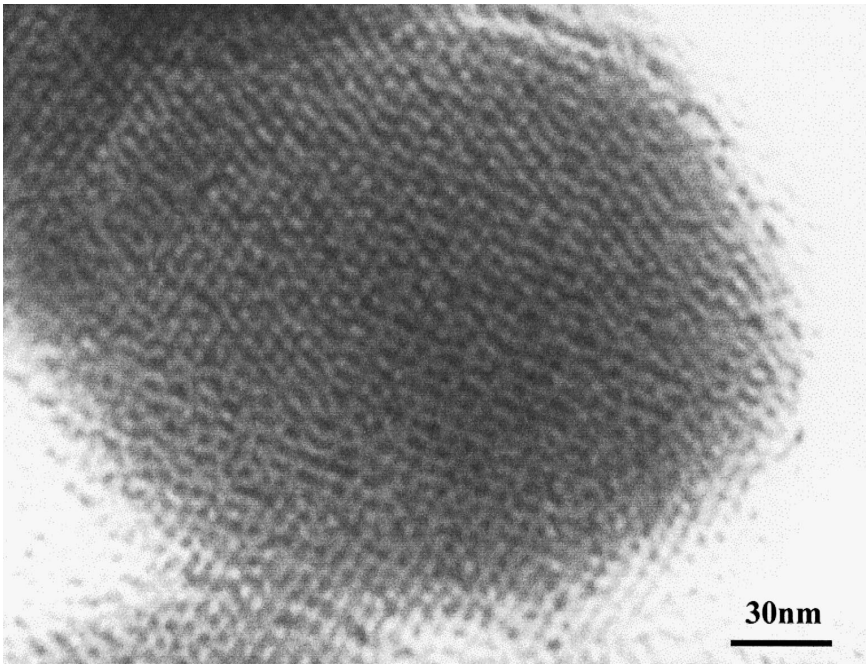

Fig. 3. Transmission electron micrograph of MCM-48 indicated the well-ordered pore structure.

hydrothermal treatment, which produces highly ordered material, has been reported for M41S molecular sieves [15]. We have found that this method for the synthesis of MCM-48 improves the stability to template removal. As with MCM-41, it is expected that lowering the pH during synthesis by replacing the mother liquor with water allows for more complete condensation thus providing well-ordered MCM-48 product. We found that highly ordered MCM-48 could be made reproducibly using a literature synthesis [14]. However, combining this synthesis with the hydrothermal treatment provided an even more ordered material according to powder XRD patterns. The combination of synthesis and a hydrothermal treatment procedure requires further optimization. Optimization of parameters such as how much washing is needed or how dry the initial MCM-48 material should be prior to the hydrothermal treatment step is not known and is beyond the scope of this study. Nevertheless, it is clear that the hydrothermal treatment is effective in the synthesis of stable, well-ordered MCM-48.

Nb-TMS4 has also been investigated for the immobilization of cytochrome *c*. Nb-TMS4 is a two dimensional layered material so there should be greater uptake of the protein compared with Nb-TMS1 [1]. It was reasoned that the semiconducting and redox active properties of Nb-TMS4 could help to facilitate the electron transfer process of immobilized proteins. Additionally, there is also the possibility that a transition metal oxide host could encourage absorption of the cytochrome *c* through weak binding of the metal and protein surface. Nb-TMS4 is synthesized using a neutral alkyl amine template that binds to Nb. It is known that amine substituted porphyrins bind to framework Nb in mesoporous molecular sieves [31]. Therefore, it is reasonable to assume that the surface amine groups (e.g., lysine residues) associated with cytochrome *c* might also interact with niobium. Based on these ideas, Nb-TMS4 was thought to be a good material to investigate as a support for cytochrome *c*.

The powder XRD pattern of as-synthesized Nb-TMS4 is shown in Fig. 4. Three reflections

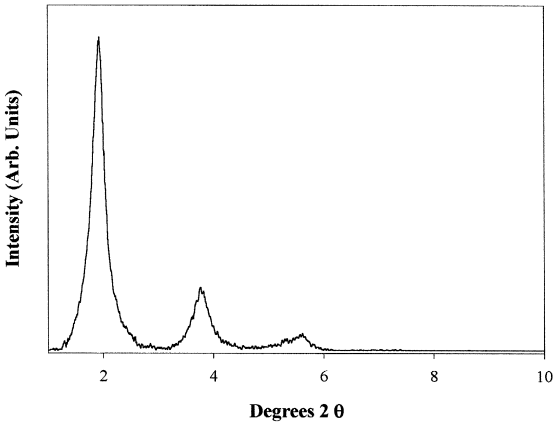

Fig. 4. Powder XRD pattern of as-synthesized Nb-TMS4 prepared by aging initial precipitate 72 h at room temperature and subsequently heating the synthesis gel in a Teflon lined autoclave for 24 h at 90°C, and 6 days at 180°C.

are observed at 1.9°, 3.8°, and 5.6° 2θ corresponding to a $d_{(100)}$ spacing of 46 Å. SEM of this material reveals an unusual rod shaped morphology, as shown in Fig. 5. The origin of this morphology is not yet clear, and to our knowledge there has been no other report of morphogenesis of Nb-TMS4. However, it has been reported that the formation of shapes such as fibers on the macroscale in silicate materials at low pH is due to fast axial growth with minimal curvature [32]. FT-IR analysis of the as-synthesized Nb-TMS4 indicates the presence of template by C—H stretching at 2919 and 2849 cm^{-1} and the metal oxide stretch, Nb—O, is observed at 1000 cm^{-1}. Having prepared highly ordered Nb-TMS4, some of the neutral amine template must be removed to gain access to the pore structure for protein immobilization. It was observed that an acidic isopropanol/water wash removes the octadecylamine template, however, repeated washings resulted in collapse of the layered structure as evidenced by powder XRD. In order to circumvent this loss of structural order, alternative template removal methods were attempted, including heating the as-synthesized Nb-TMS4 in isopropanol at 80°C for approximately 3 h [33]. This wash has been reported to be suitable for removal of neutral amine templates, however this method proved unsuccessful as well. An additional wash in 5% nitric acid solution heated to 80°C for 24 h also resulted in collapse of the Nb-TMS4. In an attempt to stabilize the layered phase structure, a post-hydrothermal treatment [34] was attempted by heating the Nb-TMS4 in 10 ml of

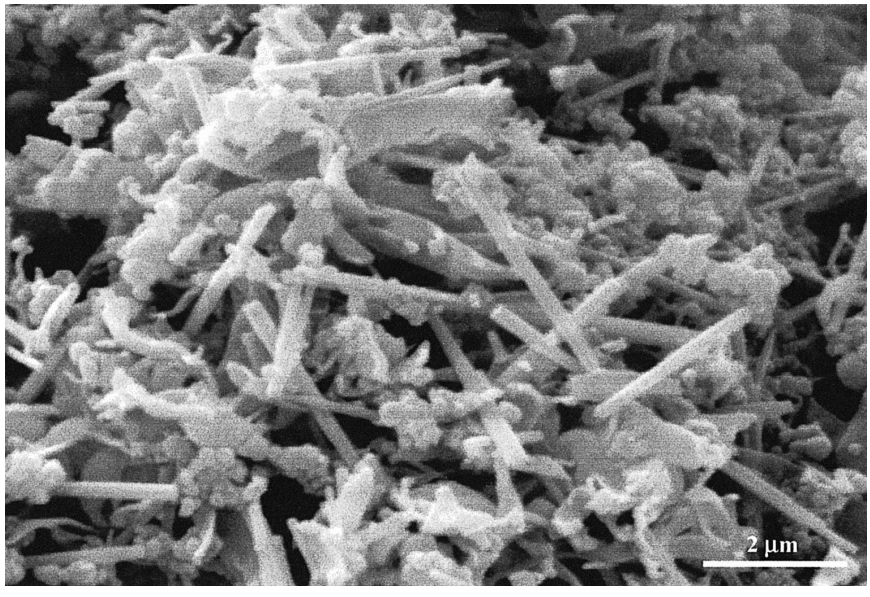

Fig. 5. Scanning electron micrograph of Nb-TMS4.

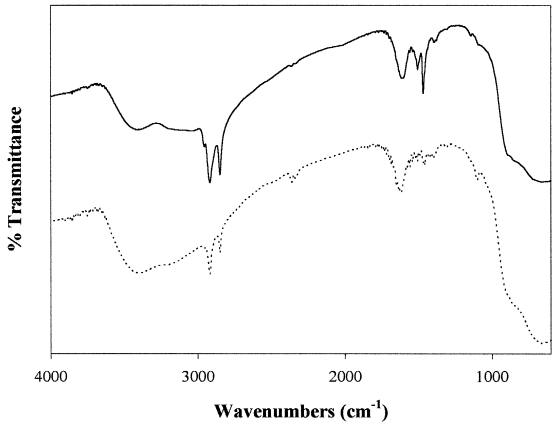

Fig. 6. FT-IR spectra of the (a) as-synthesized Nb-TMS1 (solid line) and (b) template removed Nb-TMS1 (dotted line) after nitric acid extraction.

deionized water at 180°C for 3 days, again resulting in loss of crystallinity. It appears that some templates are needed to pillar the layers and stabilize the structure. Thus, cytochrome *c* absorption experiments were carried out using Nb-TMS4 with only ~25% of the template removed as shown in Fig. 6.

All silica SBA-15 is a one-dimensional ultra-large mesoporous (50–300 Å) material with enhanced stability compared to MCM-type mesoporous materials due to the thickness of the SBA-15 pore walls. SBA-type materials are reported to have walls 31–64 Å thick [16] compared to the ~8 Å thick walls associated with MCM-type materials. Even though SBA-15 is a one-dimensional channel system, the ultra-large pores make the material attractive for the immobilization of larger biomolecules, thus we are not size-limited by the molecular sieve pore diameter. SBA-15 was characterized by powder XRD, SEM, and FT-IR. Three reflections were readily observed in the powder XRD pattern at 0.9°, 1.5°, and 1.8° 2θ for the calcined material. The pore diameter of the calcined SBA-15 is 90–110 Å as determined by argon adsorption isotherms (not shown).

3.2. Molecular sieve / cytochrome c composites

Cytochrome *c* (MW = 12,382) is a somewhat spherically shaped protein having an average molecular diameter of 30 Å. Cytochrome *c* is a basic protein and several of the lysine residues are clustered around the mouth of the heme crevice [35], which may lead to a preferred attachment to certain surfaces [36]. The active sight consists of an iron (III) porphyrin heme group, only 4% of which is exposed at the protein outer surface [18]. Based on these dimensions, the protein cytochrome *c* should easily fit inside the pores of MCM-48, as well as the other molecular sieves studied here. Additionally, the internal surface of MCM-48 is lined with terminal silanol groups [37] that likely facilitate immobilization of cytochrome *c* via hydrogen bonding.

Cytochrome *c* was readily absorbed into template removed molecular sieves by stirring in pH 7 buffered solutions ranging from 15 to 100 μM cytochrome *c* in an ice bath. Using UV/Vis spectroscopy, cytochrome *c* loading into each molecular sieve was calculated. A comparison of cytochrome *c* loading into MCM-48, Nb-TMS4, and SBA-15 is contained in Table 1. Fig. 7 shows the UV/Vis absorption spectra of a 15-μM buffered solution of cytochrome *c* before and after absorption into MCM-48. Based on the UV/Vis spectra of the supernatant after 2 h contact time with the molecular sieve, all of the detectable cytochrome *c* was absorbed by the molecular sieve, corresponding to a cytochrome *c* loading of 11.8 mg/g MCM-48. In comparison with the all silica and aluminosilicate MCM-41, cytochrome *c* loadings from 15 μM solutions under similar conditions were found to be 6.2 and 5.7 mg/g molecular sieve, respectively [1]. Thus, a significantly higher loading, ~50%, was observed for the three-dimensional material MCM-48 over the one-dimensional MCM-41

Table 1
Comparison of cytochrome *c* loadings into molecular sieves

Molecular sieve	Surface area (m^2/g)	Cytochrome *c* (mg/g)
MCM-48	1100	11.8
Nb-TMS4	< 500	6.2
SBA-15	600	8.0

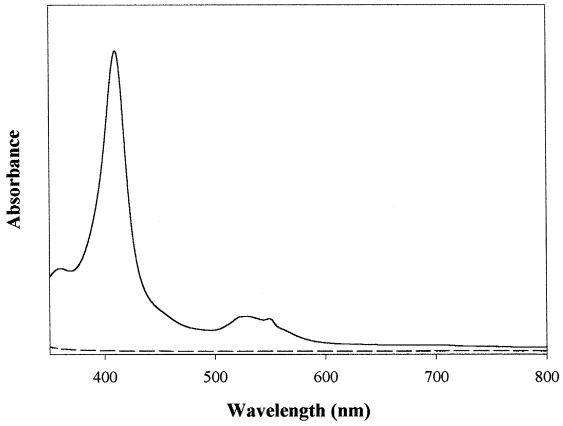

Fig. 7. UV/Vis spectra of cytochrome *c* solution (pH 6.0) (a) before absorption into MCM-48 (solid line) and (b) after absorption into MCM-48, 2 h stirring time (dashed line).

materials [1,2]. Cytochrome *c* loading into amorphous silica sol–gel has been reported in the range of 10–30 mg/g xerogel, corresponding to 93–94% overall immobilization of the protein into the sol–gel [38]. Immobilization into sol–gels was accomplished by sol polymerization in the presence of the protein [38–40]. Therefore, MCM-48 appears to be as efficient as sol–gel immobilization but has the advantage of a uniform pore structure.

During cytochrome *c* absorption into the molecular sieves, a small amount of cytochrome *c* may be adsorbed to the exterior surfaces. However, due to the high surface area of template-free molecular sieves, the vast majority of cytochrome *c* will be absorbed into the pores. In an attempt to evaluate exterior surface adsorption of the protein onto MCM-48, 5 ml of an 18-μM (1.1 mg) cytochrome *c* solution was stirred with 50 mg of as-synthesized MCM-48, which has pores completely blocked with the surfactant template. By UV/Vis spectroscopy, it was determined that only 0.5 μM (0.03 mg) cytochrome *c* was adsorbed by the MCM-48, which corresponds to a cytochrome *c* loading of 0.6 mg/g MCM-48, thus confirming that only a small portion ($< 3\%$) of the cytochrome *c* is adsorbed to the outer surfaces of the 0.5–1.0 μm molecular sieve particles.

For cytochrome *c* absorption into Nb-TMS4, solution concentrations were varied from 15 to 80 μM. From these solution, loadings of 6.2 and 23.5 mg cytochrome per gram of Nb-TMS4 were obtained, respectively. A loading of 8.0 mg cytochrome *c* per gram of SBA-15 molecular sieve was calculated using UV/Vis spectroscopy (not shown) of a 15-μm protein solution. Upon cytochrome *c* absorption into each molecular sieve, the support underwent a color change from white, before loading, to pink after protein absorption, providing physical evidence for cytochrome *c* loading. Cytochrome *c* loading differences are likely due to molecular sieve structure differences. One may expect the highest loading in MCM-48 due to the three-dimensional pore system compared to the pillared Nb-TMS4, or the one dimensional SBA-15. The order of cytochrome *c* loading also coincides with our surface area measurements, as shown in Table 1.

The intercalation of guest molecules into layered materials such as Nb-TMS4 can be characterized by powder XRD. Thus, further evidence for cytochrome *c* absorption into Nb-TMS4 may be obtained by a comparison of the powder XRD patterns of as-synthesized Nb-TMS4, acid extracted Nb-TMS4, and cytochrome *c* incorporated Nb-TMS4, as shown in Fig. 8. Upon acid extraction of Nb-TMS4, contraction of the unit

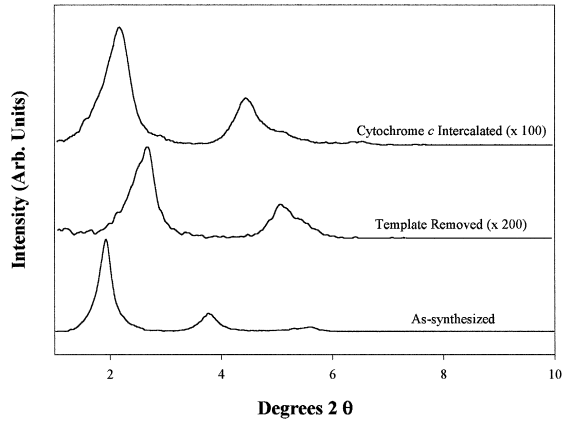

Fig. 8. Powder XRD patterns of (a) as synthesized Nb-TMS4, (b) acid extracted Nb-TMS4, and (c) cytochrome *c* incorporated Nb-TMS4.

cell is observed, with a shift in the $d_{(100)}$ spacing from 46 Å down to 33 Å. Upon cytochrome *c* intercalation into the Nb-TMS4, the (100) reflection *d*-spacing shifts back up to 41 Å, corresponding to an increase in Nb-TMS4 layer spacing upon immobilization. However, the *d*-spacing does not return to that of the as-synthesized material.

It has previously been shown that cytochrome *c* desorbs from MCM-41-type mesoporous molecular sieves at pH 10, the isoelectric point of cytochrome *c* [2]. Indeed, this same result was observed for Nb-TMS1, siliceous MCM-48, and aluminosilicate MCM-41 [2]. For each non-silane functionalized molecular sieve, the leaching of cytochrome *c* at pH ≤ 10 was very small (~ 0.3–0.5%), while the protein leakage at pH 10 was $\sim 3\%$ after submersion in a pH 10 buffer solution for times ranging from 2 h to overnight at room temperature. The small amounts of cytochrome *c* that can be removed by leaching are largely surface species, based on the amount of cytochrome *c* adsorbed to as-synthesized materials. However, to ensure that no occluded protein leaches out, the pore openings can be silane functionalized. This type of immobilization would be especially important if the composite were to be subjected to conditions under which the protein could leach out, i.e., high pH solutions.

Modification of the pore openings with organosilanes such as 4-(trichlorosilyl)-butyronitrile $(Cl)_3SiCH_2CH_2CH_2CN$, reduces the effective pore aperture, thereby entrapping the protein, as shown by the schematic representation in Fig. 9. Previously, two other silanes were used, 3-aminopropyltriethoxysilane, and 3-cyanopropyldimethylmethoxysilane. However, it was difficult to detect the amino functional group stretch as evidence for silylation using 3-aminopropyltriethoxysilane in the FT-IR spectrum. Additionally, the amino group could react to form covalent linkages whereas an organosilane containing a nitrile group would be less reactive. Using 3-cyanopropyldimethylmethoxysilane, silylation of the MCM-48 surface was achieved as evidenced by the nitrile stretch at 2257 cm^{-1}. However, the alkoxysilane proved to be less reactive than 4-(trichlorosilyl)butyronitrile, which was used in all subsequent experiments. It is estimated that the mesopore would be reduced by approximately 12 Å if two $-(O)_3SiCH_2CH_2CH_2CN$ groups are situated directly across from one another in the pore opening. Thus access to the protein is not restricted, and both small molecule (< 25 Å) diffusion as well as electron transfer is possible. During the silylation reaction, hydrochloric acid is formed, thus lowering the solution pH. While it seems that MCM-48 is stable at low

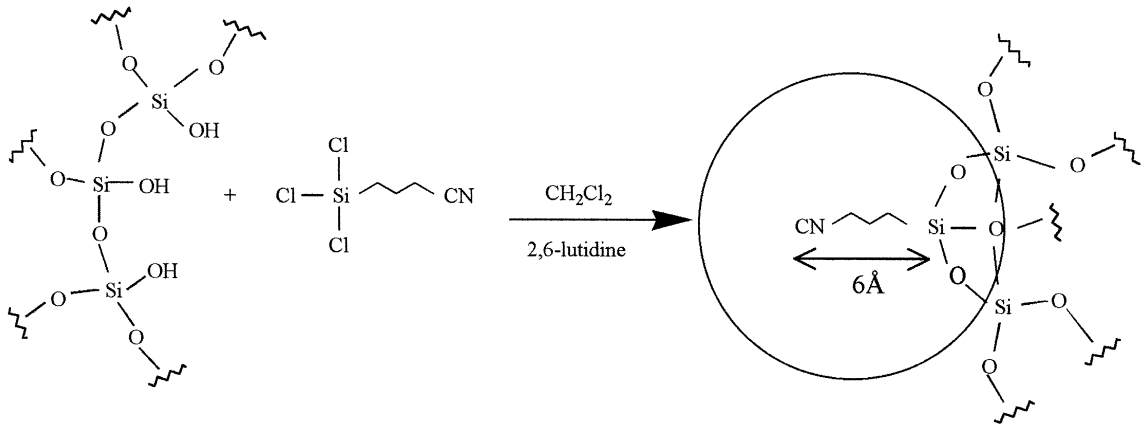

Fig. 9. Schematic representation for silylation of an all silica molecular sieve pore opening using 4-(trichlorosilyl)butyronitrile.

pH based on other work conducted in our laboratory [41], the protein may begin unfolding at low pH [42]. The addition of a non-nucleophilic base such as 2,6-lutidine to the silylation reaction regulates pH by acting as a proton scavenger. We do not anticipate silylation of the cytochrome *c* because the immobilization of proteins and enzymes into sol–gels employs similar alkoxysilanes in the presence of cytochrome *c* and does not pose a problem in such work [38]. The FT-IR spectrum shown in Fig. 10 reveals a nitrile stretch at 2257 cm^{-1}, providing evidence for attachment of the organosilane. Additionally, C–H stretching bands due to the methylene groups are observed at 2942 and 2893 cm^{-1}, and a C–H deformation band is observed at 1429 cm^{-1}. Because the silylation was performed on template-free MCM-48, the C–H stretching bands observed in Fig. 10 are attributed to the organosilanes. From an FT-IR analysis comparing ratios of the terminal silanol band in the region of 3740 cm^{-1} and the asymmetric stretch at $\sim$1091 cm^{-1}, it is estimated that $\sim$40% of the silanols have been silylated in calcined MCM-48. In comparison, organosilane functionalization of MCM-41 using $\sim$10 Å ethyleneamine derivatives resulted in 30–65% silylation of the accessible silanols [43]. Although bands associated with absorbed cytochrome *c* are not readily observed in the IR spectrum, the molecular sieve undergoes a distinct color change from white to pink upon absorption of cytochrome *c*, as previously mentioned.

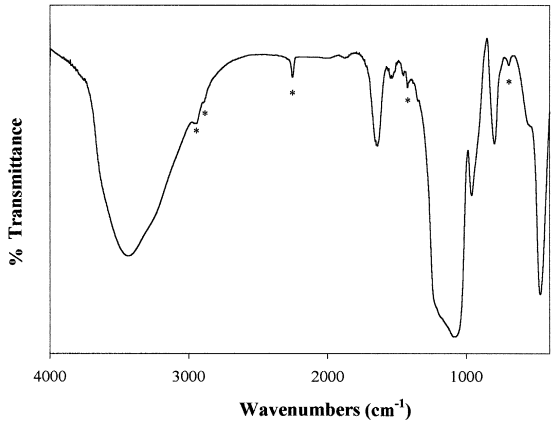

Fig. 10. FT-IR spectrum of silanated MCM-48 (* indicates peaks assigned to silane).

After silylation, the cytochrome *c* that is adsorbed on the exterior molecular sieve surface was removed by leaching in pH 10 buffer solution. Based on UV/Vis analysis, 3.9×10^{-5} g (8.4×10^{-4}%) was removed from the exterior surfaces during washing. This is a relatively small amount of protein compared with the result of cytochrome *c* adsorption to the as-synthesized material. This difference may be accounted for in protein's preference to absorb into the molecular sieve pores over the outer surface. Thus, one would expect significantly less exterior loading onto template-free molecular sieves. Additionally, some of the exterior cytochrome *c* may have been washed away during the silylation and subsequent work-up. The silane functionalized MCM-48/cytochrome *c* was stirred in fresh pH 10 buffer until no cytochrome *c* was detected in washes by UV/Vis spectroscopy. In a separate experiment, a calcined MCM-48 sample was silylated under the same conditions as the MCM-48/cytochrome *c* sample (sample did not contain cytochrome *c* prior to silylation using 4-(trichlorosilyl)butyronitrile). The silane functionalized MCM-48 sample was then stirred in an 18-μM cytochrome *c* solution. As expected by FT-IR analysis, it appears that a greater degree of silane functionalization occurs in the calcined MCM-48 material compared to the cytochrome *c* immobilized MCM-48, by comparing the ratios of the nitrile stretch and the asymmetric stretch at $\sim$1091 cm^{-1}. Upon silylation of calcined MCM-48, the silane may penetrate deep into the pores, thus allowing more surface modification compared with the cytochrome *c* immobilized MCM-48, where silylation primarily takes place at the pore openings. This is further evidenced by the absorption of 1.6 μM cytochrome *c* (determined by UV/Vis analysis) by the silylated sample of calcined MCM-48. This corresponds to 0.92 mg cytochrome *c* ab-

sorbed per gram of silylated MCM-48 which is slightly more than outer surface. This suggests the silane penetrates deeper into the pores of cytochrome *c*-free MCM-48 allowing for some protein absorption following silylation.

The edges of Nb-TMS4 were also silane-functionalized using 4-(trichlorosilyl)-butyronitrile. Silylation of cytochrome *c* containing Nb-TMS4 also required the presence of 2,6-lutidine as described for the MCM-48 experiments. If lutidine was not added to the silylation procedure, it appears that the protein is denatured, based on the lack of electrochemical activity of the Nb-TMS4/cytochrome *c* sample. No redox activity was observed by CV for the Nb-TMS4/cytochrome *c* that was silylated in the absence of 2,6-lutidine. High pH leaching of the silane functionalized Nb-TMS4/cytochrome *c* materials was carried out to remove exterior surface adsorbed protein. Virtually no leakage was observed at pHs below the protein's isoelectric point as expected, while only a small amount ($<8\%$) of leakage was observed using pH 10 buffer solution for the normal loadings, while at highest cytochrome *c* loadings, significantly more cytochrome *c* was leached ($\sim$ 30%). Fresh buffer solutions were added to the silylated Nb-TMS4 and stirred until no further cytochrome *c* desorption was detected by UV/Vis analysis. From an initial cytochrome *c* loading of 20.3 mg/g Nb-TMS4 (0.092 μmol cytochrome *c* absorbed into 50 mg sample), pH 10 leaching experiments removed 0.02, 0.005, 0.003, 0.002 μmol cytochrome *c* at 24-, 48-, 72-, and 96-h time intervals, respectively. Finally, after 116 h in a pH 10 solution, no cytochrome *c* was leached. This suggests that it is more difficult to immobilize the protein in a layered material. Silylation of SBA-15/cytochrome *c* composites using 3-cyanopropyldimethylmethoxysilane was confirmed by FT-IR spectroscopy. Subsequently, in a 36-h pH 10 leaching experiment, 0.32 μM (0.02 mg) of cytochrome *c* was leached from the silylated SBA-15, corresponding to approximately 2% loss of the protein from SBA-15.

Hemoproteins function in primarily three ways, transport and storage of oxygen, electron transport, and the oxidation of substrates. Cytochrome *c* is present in all organisms possessing mitochondrial respiratory chains and serves as an electron carrier [34]. The active site is an iron porphyrin, a small portion of which is exposed at the protein surface. The Fe(II)/(III) redox couple provides for convenient characterization by electrochemical methods. In fact, cytochrome *c* may be the most widely studied of all metalloproteins with respect to its electrochemical properties [35,44–54]. However, relatively few results have been published concerning the electrochemistry of immobilized cytochrome *c* [36,49–53]. The CV of solution cytochrome *c* in the presence of 4,4′-bipyridyl and its derivatives as a diffusable electron transfer mediator has been the most popular system studied [46,48,53,54] and was used in our CV studies of molecular sieve immobilized cytochrome *c*.

The CV results obtained at a scan rate of 150 mV/s from cytochrome *c* immobilized into MCM-48 exhibit a single oxidation and reduction process, with the anodic peak at 0.19 V and the cathodic peak at 0.13 V vs. Ag/AgCl ($E_{1/2}$ = 0.16 V) as shown in Fig. 11A, corresponding to a redox potential of 0.36 V vs. Normal Hydrogen Electrode (NHE). This shift is consistent with immobilization of cytochrome *c* onto an interacting support (vide infra) [51,52]. Additionally, there does appear to be the possibility of a reduced species at low potential, at -0.13 V in Fig. 11A. Ferricytochrome *c* undergoes an alkaline conformational change at around pH 9 [55] and exhibits a reversible couple at -0.205 V vs. NHE [56]. Thus, the apparent peak could be due to the reduction of alkaline cytochrome *c* due to the high pH washings following silylation. However, the extent to which cytochrome *c* is mobile and able to make conformational changes within the smaller pore MCM-48 and Nb-TMS4 is not known. There is no other evidence in the electrochemical data for all other samples to support a high pH cytochrome

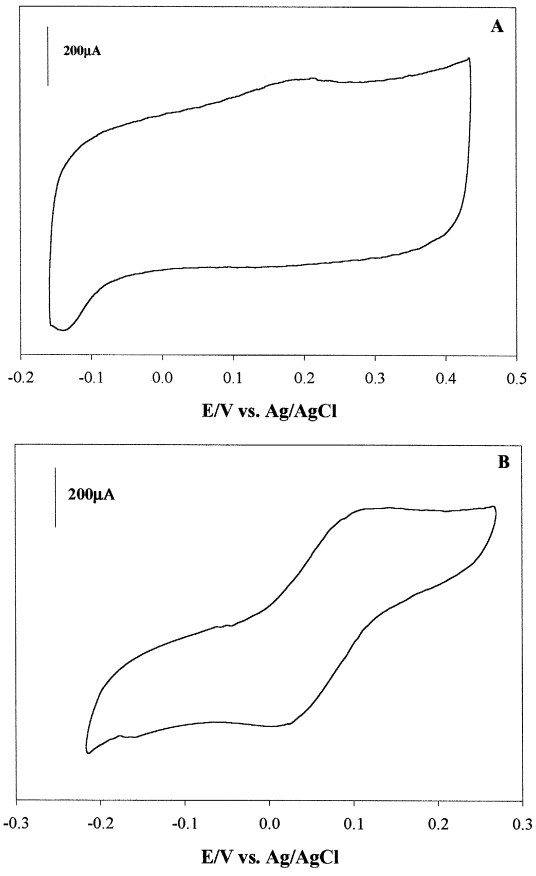

Fig. 11. Cyclic voltammograms for cytochrome *c* (A) encapsulated into MCM-48 and (B) 100 μM solution.

c conformational change. No Faradaic signal was observed from controls such as pressed carbon electrodes or a silylated MCM-48 and carbon composite electrode. Upon removal of the molecular sieve/cytochrome *c* electrode, no redox behavior was observed from solution consistent with the spectroscopic results that show the protein was trapped in the molecular sieve pores. Therefore, the observed electrochemical response arises from the entrapped protein, and is not attributed to leakage of the protein into the solution or the carbon. The reduction of 4,4′-bypyridyl was observed at much lower potentials, around −0.86 V vs. Ag/AgCl and does not interfere with the couple associated with cytochrome *c*. Therefore, 4,4′-bypyridyl may not function as a conventional mediator, but rather has been reported to act by adsorbing on the electrode surface to produce an interface at which rapid electron transfer is possible [35]. The reduction and oxidation of a 100-μM solution of purified cytochrome *c* is shown in Fig. 11B. The anodic and cathodic peaks are observed at 94 and 26 mV vs. Ag/AgCl, respectively, ($E_{1/2} = 60$ mV) corresponding to a potential of 257 mV vs. NHE, in good agreement with the reported cytochrome *c* redox potential of 260 mV vs. NHE.

We have previously reported the observation of two redox couples in the hexagonal niobium metal oxide, Nb-TMS1, containing cytochrome *c* [1]. It was postulated that the source of the second couple was impurities in the as-received cytochrome *c*. Therefore, the cytochrome *c* was purified as described above for immobilization into the layered material, Nb-TMS4. However, subsequent immobilization of fresh solutions of as-received cytochrome *c* did not provide two redox couples. In a separate experiment, as-synthesized Nb-TMS4 was also stirred in a solution of purified cytochrome *c*, and the CV of the solution was taken to determine if contact with the Nb-TMS1 surface was causing the apparent denaturing of the cytochrome *c* protein or even promoting the conformational change. Results of this experiment showed a single quasireversible couple where the anodic peak occurs at 102 mV and the cathodic peak occurs at 0 mV vs. Ag/AgCl, indicating that the niobium oxide support was not the cause of the denaturing. Eventually, it was discovered that a purified cytochrome *c* solution aged for 2 days in phosphate buffer at −4°C, and subsequently immobilized into Nb-TMS4, produced two quasireversible redox couples. Anodic peaks occurred at −0.02 and +0.28 V and the corresponding cathodic peaks occurred at −0.07 and +0.26 V. Therefore, storing the solution before immobilization results in some denaturation of the cytochrome *c*, which produces the second redox couple. In contrast, cytochrome *c* immobilized in Nb-TMS4 or MCM-48 can be stored for weeks without denaturing. Even protein ex-

tracted from the non-silylated molecular sieve that has been heated to 120°C shows no sign of denaturing. These results demonstrate the stability advantage of immobilizing or even storing the proteins in molecular sieves. Electrochemical characterization of purified cytochrome *c* in Nb-TMS4 at a scan rate of 150 mV/s reveals one redox couple having the anodic peak at 0.16 V and the cathodic peak at 0.09 V vs. Ag/AgCl ($E_{1/2} = 0.13$ V), corresponding to a redox potential of 0.33 V vs. NHE, as shown in Fig. 12. These results are similar to those observed in MCM-48, with a smaller shift of the observed cytochrome *c* redox potential in Nb-TMS4 compared to that observed in the all silica MCM-48. Due to the relatively small mesopore and layer spacing afforded by MCM-48 and Nb-TMS4, we investigated the ultra-large mesoporous material SBA-15. While SBA-15 has only one-dimensional channels, the large pores of SBA-type materials allows for the immobilization of cytochrome *c* as well as significantly larger biomolecules into the mesoporous molecular sieve. Additionally, the redox potential of SBA-15 containing cytochrome *c* was measured (not shown) and the anodic and cathodic peaks were observed at 0.14 and 0.09 V, respectively, at a scan rate of 125 mV/s ($E_{1/2} = 0.12$ V).

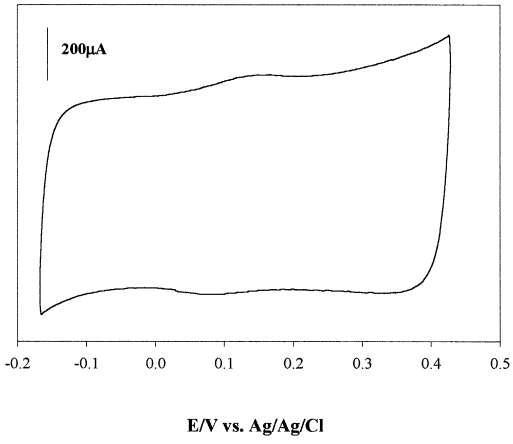

Fig. 12. Cyclic voltammogram for cytochrome *c* encapsulated into Nb-TMS4.

It is presumed that the shift in the observed potential for cytochrome *c* immobilized in each of the molecular sieves is related to the interaction of cytochrome *c* with the surface of the molecular sieve host. At a scan rate of 100 mV/s, the shift in the redox potential of the immobilized cytochrome *c* compared to the potential measured for cytochrome *c* in solution is +0.06, +0.06, and +0.10 V for SBA-15, Nb-TMS4, and MCM-48, respectively. Shifts in redox potentials of immobilized cytochrome *c* (covalently bound) onto glassy carbon electrodes range from −45 to +74 mV. Positive shifts have been related to protein conformational changes upon immobilization that increases the energy of the conformational transition from the oxidized to the reduced form [51,52]. One would expect the numerous lysine residues at the protein surface to hydrogen bond with the terminal silanol groups on the molecular sieve surface. However, because the all silica materials MCM-48 and SBA-15 are significantly more acidic than the niobium oxide Nb-TMS4, it can be expected that the basic cytochrome *c* molecule would interact more with the silica hosts than with more basic Nb-TMS4. Spectroscopic evidence for protein binding to the Nb was obscured by the template required to pillar the Nb-TMS4 material. Host molecular sieve pore size must also affect the degree of interaction with cytochrome *c*. The MCM-48 pore diameter (32–35 Å) is similar to Nb-TMS4 layer spacing, while SBA-15 has a much larger pore size (~100 Å). Thus, the largest shift in redox potential is observed in MCM-48, while SBA-15 and Nb-TMS4 show very similar shifts in redox potential compared to solution cytochrome *c*. Therefore, it appears that the large pore size associated with SBA-15 reduces the interaction of cytochrome *c* with the silica surface even though it is compositionally the same as the smaller pore MCM-48, resulting in the Fe(II/III) potential for cytochrome *c* to be very close to that observed in Nb-TMS4.

The molecular sieve/carbon composite electrodes produce a relatively small signal, which

is attributed to the insulating nature of MCM-48 and SBA-15 as well as the semiconducting character of Nb-TMS4. Another contributing factor to the smaller electrochemical signal includes the lower concentration of cytochrome *c* in the molecular sieve compared to solution electrochemistry experiments. Further, it is not known how much of the cytochrome *c* molecules are oriented in the pores in a manner that facilitates electron transport. However, it has been previously shown that upon immobilization of cytochrome *c* onto a carbon glassy electrode, the protein molecule orients in only one electroactive position in the presence of an electric field [36]. In this orientation, the protein surface appears almost flat. In the case of cytochrome *c* encapsulated into MCM-48, the host is a highly curved surface, instead of flat one. However, the Nb-TMS4 layered material is much flatter than MCM-48, and the large SBA-15 pores may present a flatter surface to the protein than the smaller MCM-48 material. In any case, it seems that the orientation of the cytochrome *c* active site could be controlled through use of techniques such as those reported in the literature [36] to maximize the immobilized protein activity, and thereby improve this system. As seen in Figs. 11A and 12, the anodic peak is more defined than the cathodic peak. This observation has been previously reported for cytochrome *c* that was covalently bound to a glassy carbon electrode, and has been attributed to the degree of irreversibility of the electrochemical reaction [36]. Table 2 contains representative redox couples for MCM-48, Nb-TMS4, and SBA-15 immobilized cytochrome *c*. Despite these factors, it is clear that cytochrome *c* remains intact following immobilization into a variety of mesoporous molecular sieves.

Table 2
Representative CV results of encapsulated cytochrome *c*

	Ox potential (V)	Red potential (V)	ΔE_p	$E_{1/2}$	vs. NHE
Purified cytochrome c					
75 mV/s	0.096	0.023	0.073	0.060	0.257
100 mV/s	0.093	0.026	0.067	0.060	0.257
125 mV/s	0.096	0.016	0.080	0.056	0.253
MCM-48 / cytochrome c					
50 mV/s	0.16	0.14	0.02	0.15	0.35
100 mV/s	0.17	0.13	0.04	0.15	0.35
150 mV/s	0.19	0.13	0.06	0.16	0.36
SBA-15 / cytochrome c					
50 mV/s	0.13	0.09	0.04	0.11	0.31
75 mV/s	0.13	0.09	0.04	0.11	0.31
100 mV/s	0.14	0.09	0.05	0.12	0.32
125 mV/s	0.14	0.09	0.05	0.12	0.32
Nb-TMS4 / cytochrome c					
100 mV/s	0.15	0.09	0.06	0.12	0.32
150 mV/s	0.19	0.09	0.10	0.14	0.34
200 mV/s	0.18	0.08	0.10	0.13	0.33

4. Conclusions

The encapsulation and immobilization of small biomolecules such as cytochrome *c* into a variety of mesoporous molecular sieves such as MCM-48 and SBA-15 and the layered transition metal oxide Nb-TMS4 has been clearly shown by UV/Vis spectroscopy, FT-IR, and CV studies. Cytochrome *c* loading into the various molecular sieves is influenced by the structure of the molecular sieve and the surface area of each material. Greater protein loading was observed for the three-dimensional MCM-48 compared to the one-dimensional hexagonal SBA-15 and two-dimensional layered Nb-TMS4. Further MCM-48 showed the highest surface area of the three materials investigated, which undoubtedly has an influence on cytochrome *c* loading. Electrochemical characterization of the entrapped cytochrome *c* verifies that the protein retains activity upon encapsulation and immobilization. The effect of pore size and layer spacing on the case of electron transfer (i.e., comparing large pore SBA-15 and smaller materials such as MCM-48 and Nb-TMS4) remains to be studied. The fabrication of mesoporous molecular sieve films provides a method for the immobilization of biomolecules into supported films.

Acknowledgements

We thank Claire Bambrough for acquiring argon adsorption data. We also thank the National Science Foundation and the Robert A. Welch Foundation for financial support of this project.

References

[1] M.E. Gimon-Kinsel, V.L. Jimenez, L. Washmon, K.J. Balkus Jr, Stud. Surf. Sci. Catal. 117 (1998) 373.
[2] J.F. Diaz, K.J. Balkus Jr, J. Mol. Catal. B: Enzym. 2 (1996) 115.
[3] W. Hartmeier, Immobilized Biocatalysts, Springer-Verlag, Berlin, 1988.
[4] A. Corma, Q. Dan, F.J. Rey, J. Chem. Soc. Chem. Commun. (1998) 579.
[5] A.A. Romero, M.D. Alba, W. Zhou, J. Klinowski, J. Phys. Chem. B 101 (1997) 5292.
[6] P. Van Der Voort, M.M.F. Mees, E.F. Vansant, J. Phys. Chem. B 102 (1998) 8847.
[7] S. Kawi, M. Te, Catal. Today 44 (1998) 101.
[8] C.T. Kresge, M.E. Leonowicz, W.J. Roth, J.C. Vartulli, J.S. Beck, Nature 369 (1992) 710.
[9] Data file courtesy of M.W. Anderson, UMIST, Manchester, M60 1QD, England.
[10] D.M. Antonelli, A. Nakahira, J.Y. Ying, Inorg. Chem. 35 (1996) 3126.
[11] L. Zhang, T. Sun, J.Y. Ying, J. Chem. Soc., Chem. Commun. (1999) 1103.
[12] D. Zhou, J. Feng, Q. Huo, N. Melosh, G.H. Fredickson, B.F. Chmelka, G.D. Stucky, Science 279 (1998) 548.
[13] F. Bedioui, E. De Boysson, J. Devynck, K.J. Balkus Jr, J. Chem. Soc. Faraday Trans. 87 (1991) 3831.
[14] J. Xu, Z. Luan, H. He, W. Zhou, L. Kevan, Chem. Mater. 10 (1998) 3690.
[15] L. Chen, T. Horiuchi, T. Mori, K. Meada, J. Phys. Chem. B 103 (1999) 1216.
[16] D. Zhao, Q. Huo, J. Feng, B.F. Chmelka, G.D. Stucky, J. Am. Chem. Soc. 120 (1998) 6024.
[17] D.L. Brautigan, S. Ferguson-Miller, E. Margoliash, Methods Enzymol. 53D (1978) 128.
[18] B. Durham, F.S. Millett, in: R.B. King (Ed.), Encyclopedia of Inorganic Chemistry Vol. 4 Wiley, Chischester, 1994.
[19] J.S. Beck, J.C. Vartulli, W.J. Roth, M.E. Leonowicz, C.T. Kresge, K.D. Schmitt, C.T.-W. Chu, D.H. Olson, E.W. Sheppard, S.B. McCullen, J.B. Higgins, J.L. Schlenker, J. Am. Chem. Soc. 114 (1992) 10834.
[20] D. Brunel, A. Cauvel, F. Fajula, F. DiRenzo, Stud. Surf. Sci. Catal. 97 (1995) 173.
[21] K. Moller, T. Bein, Chem. Mater. 10 (1998) 2590.
[22] D. Sheng, M.C. Burleigh, Y. Shin, C.C. Morrow, C.E. Barnes, Z. Xue, Angew. Chem., Int. Ed. 38 (1999) 1235.
[23] S. O'Brien, J.M. Keates, S. Barlow, M.J. Drewitt, B.R. Payne, D. O'Hare, Chem. Mater. 10 (1998) 4088.
[24] M.J. MacLachlan, P. Aroca, N. Coombs, I. Manners, G.A. Ozin, Adv. Mater. 10 (1998) 144.
[25] X.S. Zhao, G.Q. Lu, J. Phys. Chem. B 102 (1998) 1556.
[26] D.S. Shephard, W. Zhou, T. Maschmeyer, J.M. Matters, C.L. Roper, S. Parsons, B.F.G. Johnson, M.J. Duer, Angew. Chem., Int. Ed. 37 (1998) 2719.
[27] M. Park, S. Komarneni, Microporous Mesoporous Mater. 25 (1998) 75.
[28] K.A. Koyano, T. Tatsumi, Y. Tanaka, S. Nakata, J. Phys. Chem. B 101 (1997) 9436.
[29] N.R.E.N. Impens, P. van der Voort, E.F. Vansant, Microporous Mesoporous Mater. 28 (1999) 217.
[30] R. Schmidt, M. Stöcker, D. Akporiaye, E.H. Tørstad, A. Olsen, Microporous Mater. 5 (1995) 1.
[31] J.Y. Ying, C.P. Mehnert, M.S. Wong, Angew. Chem., Int. Ed. (38) (1999) 56.
[32] N. Coombs, D. Khushalani, S. Oliver, G.A. Ozin, G.C. Shen, I. Sodolov, H. Yang, J. Chem. Soc., Dalton Trans. (1997) 3941.
[33] D.L. Macquarrie, J. Chem. Soc., Chem. Commun. (1996) 1961.
[34] R. Ryoo, J.M. Kim, J. Chem. Soc., Chem. Commun. (1995) 711.
[35] L.-H. Guo, H.A.O. Hill, Advances in Inorganic Chemistry Vol. 36 Academic Press, 1991, p. 341.
[36] B.A. Kuznetsov, N.A. Byzova, G.P. Shumakovich, J. Electroanal. Chem. 371 (1994) 85.
[37] H. Landmesser, H. Kosslick, W. Storeck, R. Frike, Solid State Ionics 101–103 (1997) 271.
[38] I. Gill, A. Ballesteros, J. Am. Chem. Soc. 120 (1998) 8587.
[39] D. Avnir, S. Braun, O. Lev, M. Ottolenghi, Chem. Mater. 6 (1994) 1605.
[40] E.H. Lan, B.C. Dave, J.M. Fukuto, B. Dunn, J.I. Zink, J.S. Valentine, J. Mater. Chem 9 (1999) 45.
[41] L. Washmon-Kriel, K.J. Balkus, Jr., in preparation.
[42] J.B. Wooten, J.S. Cohen, I. Vig, A. Schejter, Biochemistry 20 (1981) 5394.
[43] J.F. Diaz, K.J. Balkus Jr., F. Bedioui, V. Kurshev, L. Kevan, Chem. Mater. 9 (1997) 61.
[44] S.R. Betso, M.H. Klapper, L.B. Anderson, J. Am. Chem. Soc. 94 (1972) 8197.
[45] M.J. Eddowes, H.A.O. Hill, J. Chem. Soc., Chem. Commun. (1977) 722.
[46] P. Yeh, T. Kuwana, Chem. Lett. (1977) 1145.
[47] F. Scheller, M. Jänchen, G. Etzold, H. Will, Bioelectrochem. Bioenerg. 1 (1974) 478.
[48] E.F. Bowden, F.M. Hawkridge, J.F. Chlebowski, E.E. Bancroft, C. Thorpe, H.N. Blount, J. Am. Chem. Soc. 104 (1982) 7641.
[49] J.M. Cooper, K.R. Greenough, C.J. McNeil, J. Electroanal. Chem. 374 (1993) 267.
[50] R. Akasaka, T. Mashino, M. Hirobe, J. Chem. Soc., Perkins Trans. 1 (1994) 1817.
[51] O. Ikeda, M. Ohtani, T. Yamaguchi, A. Komura, Electrochim. Acta 43 (1998) 833.

[52] Y. Zhu, J. Li, S. Dong, J. Chem. Soc., Chem. Commun. (1996) 51.
[53] M.J. Eddowes, H.A.O. Hill, Faraday Discuss. Chem. Soc. 74 (1982) 331.
[54] N.S. Lewis, M.S. Wrighton, Science 211 (1981) 944.
[55] I. Bertini, H.B. Gray, S.J. Lippard, J.S. Valentine, Bioinorganic Chemistry, University Science Books, Sausalinto, 1994, p. 352.
[56] P.D. Barker, A.G. Mauk, J. Am. Chem. Soc. 114 (1992) 3619.